

CrossMark  
click for updatesCite this: *Catal. Sci. Technol.*, 2016,  
6, 4695Received 11th January 2016,  
Accepted 3rd February 2016

DOI: 10.1039/c6cy00070c

www.rsc.org/catalysis

A novel macromolecular photoredox catalyst based on  $[\text{Ru}(\text{bpy})_3]^{2+}$  anchored to a 2nd-generation PAMAM dendrimer has been developed. Its catalytic activity under visible light irradiation and recyclability using organic solvent nanofiltration with a size-exclusion membrane have been explored under continuous flow conditions.

Visible-light photoredox catalysis has recently emerged as a very powerful tool for organic synthesis.<sup>1</sup> These methods rely on the redox properties of so-called photoredox catalysts upon absorption of low energy visible light. The single-electron transfer processes triggered by catalyst irradiation permits the construction of bonds (especially C–C bonds) difficult to achieve by conventional means, and in many instances avoids the use of stoichiometric amounts of oxidants or reductants.<sup>1</sup> The use of visible light instead of UV prevents deterioration of substrates and products in the reaction mixture, and constitutes a greener method of activation. Notably, this synthetic method has been shown as a valuable tool in the preparation of complex molecules and natural products such as heitziamide A<sup>2</sup> and aplyviolene.<sup>3</sup> The most commonly used photoredox catalysts are ruthenium and iridium polypyridyl complexes. Tris(2,2'-bipyridine) ruthenium(II) ( $[\text{Ru}(\text{bpy})_3]^{2+}$ ) (Fig. 1) is probably the most popular catalyst and a plethora of transformation using this additive have been reported.<sup>1</sup> Ruthenium and iridium are scarce elements and the cost of these metal complexes can be considered a major drawback of photoredox catalysis. Moreover, the use of potentially toxic metals is an important concern in API synthesis, and meticulous purification procedures are typically required to meet the specification limits for metal residues. Several organic photosensitizers have been reported to substitute the use of

## Visible-light photoredox catalysis using a macromolecular ruthenium complex: reactivity and recovery by size-exclusion nanofiltration in continuous flow†

Javier Guerra,<sup>ab</sup> David Cantillo<sup>a</sup> and C. Oliver Kappe<sup>\*a</sup>

ruthenium or iridium compounds in some instances.<sup>4</sup> Yet, most transformations being reported still rely on the photoredox catalysis properties of  $[\text{Ru}(\text{bpy})_3]^{2+}$ .<sup>1</sup>

Photochemistry in general and photoredox catalysis in particular have benefited from technological advances such as the use of continuous flow reactors.<sup>5</sup> The relatively low reactor volume and in particular the high surface to volume ratio of capillary flow reactors assure intense and uniform irradiation of the reaction mixture. Important reaction enhancements including reduced reaction times and catalyst loadings have been described for  $[\text{Ru}(\text{bpy})_3]^{2+}$  and related systems.<sup>5</sup> However, catalyst loadings of 0.5–1 mol% are still typically required.

There is therefore little doubt that development of catalyst recovery/recycling technology for metal-based photoredox catalysts is highly desirable. In the context of continuous flow chemistry several recycling techniques for metal catalysts have been reported in the literature.<sup>6</sup> These include catalyst immobilization, liquid–liquid biphasic conditions, or organic solvent nanofiltration. Solvent nanofiltration typically requires “enlargement” of the catalyst.<sup>6</sup> Different soluble platforms such as dendrimers, polymers and polyhedral silesquioxanes have been used to anchor metal centers, in most cases palladium catalysts for cross-coupling chemistry. An example of continuous recovery/recycling of a ruthenium Grubbs–Hoveyda type catalyst anchored on a polyhedral

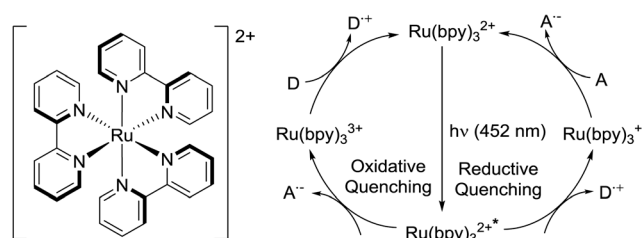


Fig. 1 Structure of  $[\text{Ru}(\text{bpy})_3]^{2+}$  and its oxidative and reductive quenching cycles.

<sup>a</sup> Institute of Chemistry, University of Graz, NAWI Graz, Heinrichstrasse 28, A-8010 Graz, Austria. E-mail: oliver.kappe@uni-graz.at

<sup>b</sup> Crystal Pharma, Gadea Pharmaceutical Group, a division of AMRI, Parque Tecnológico de Boecillo, Valladolid, 47151, Spain

† Electronic supplementary information (ESI) available: Experimental procedures, characterization data, and supplementary figures and tables. See DOI: 10.1039/c6cy00070c

oligomeric silsesquioxane for ring metathesis was described by Grela.<sup>7</sup> Bergbreiter and coworkers prepared a modified recyclable  $\text{Ru}(\text{bpy})_3^{2+}$  based photocatalyst decorated with multiple polyisobutene chains, that could be separated by selective precipitation from the reaction mixture.<sup>8</sup> More recently, the group of Reiser has described a continuous flow procedure for the use and recycling of a polyisobutene immobilized  $\text{fac-Ir}(\text{ppy})_3$  complex.<sup>9</sup> Constant conversions with only minor losses of catalyst could be achieved using a biphasic system.<sup>9</sup> Recycling of a fluorinated photocatalyst using a biphasic system with supercritical  $\text{CO}_2$  has also been reported.<sup>10</sup> However, to the best of our knowledge, merger of organic solvent nanofiltration and photoredox catalysis using a macromolecular metal catalyst has never been described.

On the basis of all the above, we envisaged a strategy for the continuous flow utilization and in-line recycling of a ruthenium bipyridyl-based macromolecular photoredox catalyst (Fig. 2). To achieve this goal, we synthesized a second-generation polyamidoamine (PAMAM) dendrimer<sup>11</sup> decorated with bipyridine pendant ligands to which  $\text{Ru}(\text{bpy})_2^{2+}$  was attached. The resulting macromolecular  $\text{Ru}(\text{bpy})_3^{2+}$  catalyst was used for a set of model photoredox catalysis reactions under continuous flow conditions, using a photoreactor equipped with blue (450 nm) LEDs. After the reactions, the catalyst could be retrieved from the reaction mixture and recycled by continuous solvent nanofiltration with a size-exclusion membrane. Herein we report on the synthesis of the dendrimer immobilized ruthenium catalyst, its properties as photoredox catalyst, and the recovery/recycling of the dendrimer using organic solvent nanofiltration.

As platform for the construction of our macromolecular  $\text{Ru}(\text{bpy})_3^{2+}$  catalyst a second-generation polyamidoamine (PAMAM) dendrimer was chosen.<sup>11,12</sup> We used the 16 primary

amino groups located at the periphery of the dendrimer to introduce the  $[\text{Ru}(\text{bpy})_3]^{2+}$  moieties, following an analogous synthetic route to that reported by Abruña *et al.*<sup>12</sup> and Velders *et al.*<sup>13</sup> (Scheme 1). The bipyridine pendant ligand 4 was constructed following a methodology previously reported from 4,4'-dimethyl-2,2'-dipyridyl 1 and bromo dioxolane 3.<sup>12,13</sup> Attachment of the bipyridine to the dendrimer surface was carried out by imination of the dendrimer amino groups with 4 followed by reduction (Scheme 1).<sup>14</sup> Purification of the bipyridine dendrimer derivative was performed by nanofiltration using a size-exclusion membrane (NF080105, Solsep BV, The Netherlands) installed in a modified commercial continuous liquid-liquid separator (Zaiput) (Fig. S2†). This procedure facilitates the removal of reactants or byproducts with a molecular weight lower than 1 kDa. A Kaiser test was performed after the bipyridine coupling and purification to rule out the presence of free primary amines (Fig. S1†). Chelation of the Ru was performed following previous methodologies.<sup>12,13</sup> Purification of the resulting G2-PAMAM-Ru dendrimer was again carried out by continuous nanofiltration in methanol. The final G2-PAMAM-Ru catalyst was characterized by means of NMR, MALDI-TOF, ICP-MS as well as UV-visible spectroscopy measurements (see ESI† for details). Notably, ICP-MS analysis revealed that the catalyst contained an average of 14.7 Ru atoms per dendrimer unit. Measurement of the absorptivity coefficient by UV-visible spectroscopy agreed with this value (see ESI† for details).

The catalytic efficiency of our macromolecular catalyst was tested for three model photochemical reactions: the phosphine-free Appel reaction, reductive opening of chalcone epoxide and azide reduction. These reactions have been previously used as model for benchmarking studies with  $\text{Ru}(\text{bpy})_3^{2+}$  under continuous flow.<sup>15</sup> The continuous flow photochemical reactions were performed in a Vapourtec EasyMedChem instrument with a UV150 photochemical reactor (FEP tubing, 1.0 mm id, 10 mL volume) equipped with a 450 nm blue LED (Fig. S5†). The reaction mixtures were introduced into the reactor using sample loops after the system had been stabilized pumping solvent through the system at the desired flow rate.

The first transformation attempted with our catalytic system was the phosphine-free Appel reaction.<sup>16</sup> In this reaction an alcohol 6 (Table 1) is converted into the corresponding bromide 7 using  $\text{CBr}_4$  as bromine source. The classical reaction conditions require stoichiometric amounts of triphenylphosphine as reducing agent. The phosphine-free photochemical version requires the use of DMF as solvent or co-solvent as it plays a role in the reaction mechanism.<sup>17</sup> Apart from the G2-PAMAM( $\text{Ru}$ )<sub>16</sub>( $\text{PF}_6$ )<sub>32</sub> catalysts, a modified version with chloride as counteranion was also employed. The solubility of the hexafluorophosphate salt of G2-PAMAM-Ru in DMF was very poor and therefore a mixture of acetone/DMF was used (Table 1). Gratifyingly, excellent results were obtained for primary, secondary, and tertiary alcohols with both the hexafluorophosphate and chloride catalysts. Full or near to full conversion to the desired bromine derivative 7

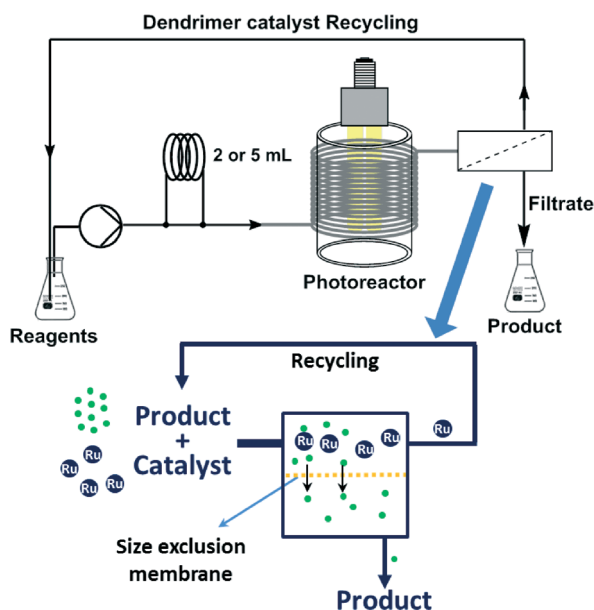
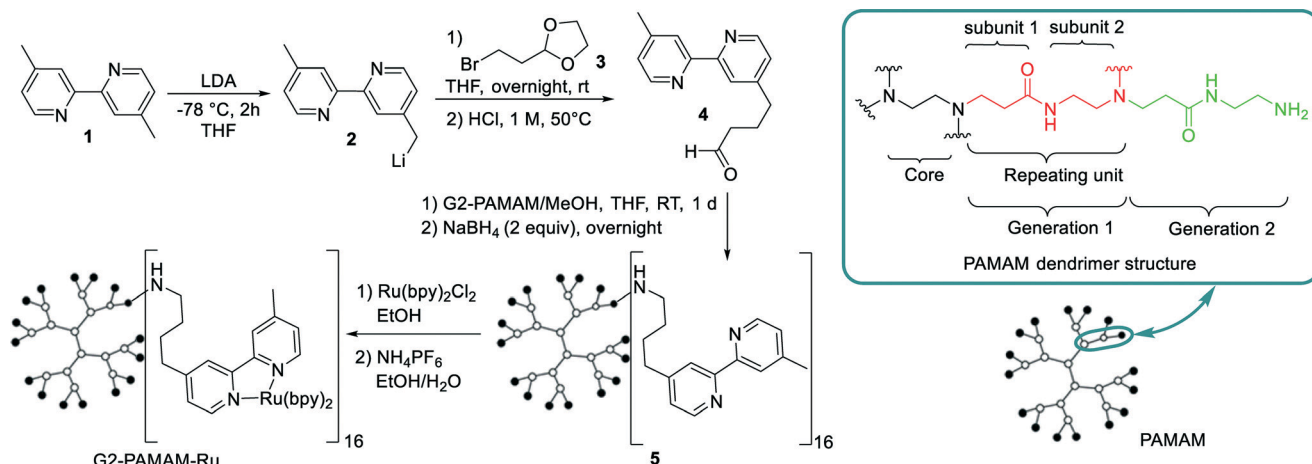


Fig. 2 Proposed setup for macromolecular photoredox catalyst use and recycling, and schematics of the continuous organic solvent nanofiltration using a size-exclusion membrane.





**Scheme 1** Synthetic sequence for the preparation of the G2-PAMAM-Ru dendrimer catalyst and detail on the PAMAM structure.

**Table 1** Catalytic activity displayed by different monomers and the dendrimer G2-PAMAM(Ru)<sub>16</sub> with hexafluorophosphate and chloride anions. Ac = acetone<sup>a</sup>

Entry	Substrate	Catalyst	Solvent	Conv. <sup>b</sup> (%)
1	1-Nonanol	Ru(bpy) <sub>3</sub> Cl <sub>2</sub>	DMF	99
2	1-Nonanol	Ru(bipy) <sub>2</sub> (Me <sub>2</sub> bpy)(PF <sub>6</sub> ) <sub>2</sub>	Ac/DMF 1 : 2	99
3 <sup>c</sup>	1-Nonanol	G2-PAMAM(Ru) <sub>16</sub> (PF <sub>6</sub> ) <sub>32</sub>	Ac/DMF 1 : 6	99
4	1-Nonanol	G2-PAMAM(Ru) <sub>16</sub> Cl <sub>32</sub>	DMF	99
5	PhCH <sub>2</sub> CH <sub>2</sub> OH	Ru(bipy) <sub>2</sub> (Me <sub>2</sub> bpy)(PF <sub>6</sub> ) <sub>2</sub>	Ac/DMF 12 : 1	94
6	PhCH <sub>2</sub> CH <sub>2</sub> OH	G2-PAMAM(Ru) <sub>16</sub> (PF <sub>6</sub> ) <sub>32</sub>	Ac/DMF 1 : 2	99
7	PhCH <sub>2</sub> OH	G2-PAMAM(Ru) <sub>16</sub> (PF <sub>6</sub> ) <sub>32</sub>	Ac/DMF 12 : 1	97
8	Ph <sub>2</sub> CHOH	G2-PAMAM(Ru) <sub>16</sub> (PF <sub>6</sub> ) <sub>32</sub>	Ac/DMF 12 : 1	99

<sup>a</sup> Conditions: 0.2 M substrate, 2 equiv. CBr<sub>4</sub>, 2 mL reaction mixture. <sup>b</sup> Determined by GC-MS. <sup>c</sup> 0.35% [Ru] was used.

was obtained in all cases, in analogy with the results obtained with the typical monomeric ruthenium catalysts (Table 1, entries 1, 2 and 5).

We chose the bromination of 1-nonanol as model to assess the photoredox catalyst recyclability. The pressure required to perform an efficient solvent nanofiltration in the presence of DMF with the membrane employed (EXP-133-LP, Solsep) was in the range from 12 to 20 bar. This pressure is above the working limit of the Vapourtec photoreactor (max. 10 bar). Thus, we decided to perform an “off-line”, continuous catalyst retrieval from the crude reaction mixture obtained from the photoreactor output using a separate syringe pump. Recycling of the G2-PAMAM(Ru)<sub>16</sub>(PF<sub>6</sub>)<sub>32</sub> catalyst was difficult due to precipitation of the catalyst and clogging of the system during filtration. This problem was not observed for G2-PAMAM(Ru)<sub>16</sub>Cl<sub>32</sub> and the filtration could be successfully carried out. Gratifyingly, ICPMS analysis of the filtrate containing the reaction product revealed that only <1% of the total ruthenium amount had been lost through

the filter. Fresh reactants were added to the obtained catalyst solution and processed in the photochemical reactor. Full conversion was again obtained. Unfortunately, when the catalyst was further recycled a drop in catalytic activity of *ca.* 20% was observed, although significant amounts of ruthenium were not detected in the filtrate (ICPMS). Visual inspection of the inner part of the liquid-liquid separator and the size-exclusion membrane (see Fig. S6†) revealed that the dendrimer catalyst had been partially retained on the membrane surface, possible due to the low solubility of the macro-molecular catalyst in the solvent mixtures employed. The decrease in catalytic activity was therefore mainly ascribed to this factor as no ruthenium was found in the filtrate.

The second set of photochemical reactions tested comprised the reductive opening of chalcone- $\alpha,\beta$ -epoxide **8** and the reduction of 4-chlorophenylazide **9** (Table 2). In both cases the HCOOH/*i*Pr<sub>2</sub>NEt reagents system was used in the absence of the Hantzsch ester as described by Seeberger.<sup>15</sup> Our G2-PAMAM-Ru dendrimer with chloride or hexafluoro-

**Table 2** Catalytic activity displayed by different monomers and dendrimer G2-PAMAM(Ru)<sub>16</sub> with hexafluorophosphate anions. Analogous results were achieved with the chloride derivative (results not shown for clarity)<sup>a</sup>

Entry	Substrate	Conc. [M]	Catalyst	Conv. <sup>b</sup> (%)
1	8	0.2	Ru(bpy) <sub>2</sub> (Me <sub>2</sub> bpy)(PF <sub>6</sub> ) <sub>2</sub>	98
2 <sup>c</sup>	8	0.2	G2-PAMAM(Ru) <sub>16</sub> (PF <sub>6</sub> ) <sub>32</sub>	99
3	9	0.1	Ru(bpy) <sub>2</sub> (Me <sub>2</sub> bpy)(PF <sub>6</sub> ) <sub>2</sub>	99
4 <sup>c</sup>	9	0.1	G2-PAMAM(Ru) <sub>16</sub> (PF <sub>6</sub> ) <sub>32</sub>	99

<sup>a</sup> Conditions: 2 mL reaction mixture, 10 equiv. HCOOH, 10 equiv. of DIPEA in MeCN. <sup>b</sup> Determined by HPLC (215 nm). <sup>c</sup> Reactions performed with only 0.6 mol% of Ru instead of 1.0 mol%.

phosphate anions delivered similar catalytic results for both reactions. Excellent conversions to the desired reduced products **10** and **11** were obtained in all cases. The efficiency was similar to that observed for the corresponding catalyst monomers (Table 2, entries 1 and 3) even employing a lower catalyst loading. Hence, anchoring on the dendrimer surface does not diminish the catalytic efficiency.

Importantly, after the epoxide and azide reductions the catalyst could be successfully retrieved from the crude reaction mixture but not reused for further catalytic cycles (a significant drop in the reaction conversion of 70% was observed after the second cycle). The decrease in catalytic activity was probably due to degradation of the dendrimeric structure in the presence of the large excess of formic acid. A specific degradation of the G2-PAMAM-Ru structure under irradiation with light cannot be discarded, as processing through the flow reactor of a solution containing only the catalyst showed a decrease in the Ru concentration after each irradiation/nanofiltration cycle. To solve this issue hydrazine hydrate was tested as reducing agent for the transformation of 4-chlorophenyl azide to the aniline (Fig. 3), using methanol as solvent. Light-mediated reduction of nitroaromatics with N<sub>2</sub>H<sub>4</sub>·H<sub>2</sub>O catalyzed by Ru(bpy)<sub>3</sub>Cl<sub>2</sub> had been previously reported,<sup>18</sup> but application to the reduction of azides constitutes a new transformation. The reaction was not as efficient as with the HCOOH/iPr<sub>2</sub>EtN system and around 50% conversion was obtained after a residence time of 20 min in the photoreactor. However, in this case the G2-PAMAM(Ru)<sub>16</sub>(Cl)<sub>32</sub> dendrimer could be recycled 5 times without apparent decrease on the catalytic efficiency.

In summary, we have described a novel macromolecular Ru(bpy)<sub>3</sub><sup>2+</sup> based dendrimeric catalyst having a high efficiency as photoredox catalyst. The catalytic activity has been tested under continuous flow conditions for a set of three model reactions displaying excellent results comparable to the common monomeric Ru(bpy)<sub>3</sub><sup>2+</sup> catalysts. The macromolecular nature of the catalysts permits its facile retrieval and recycling using size-exclusion membrane technology.

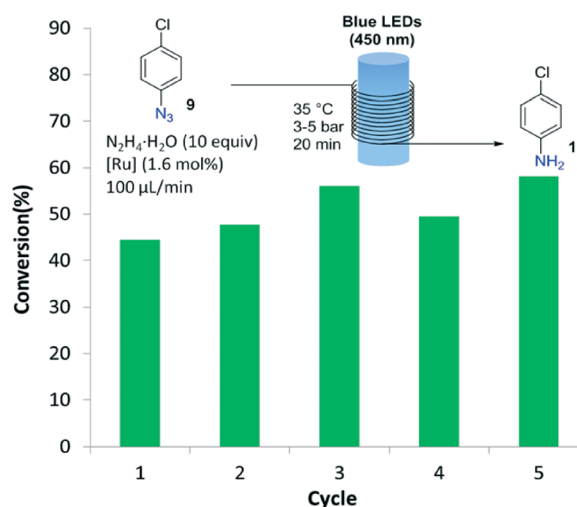


**Fig. 3** Recyclability study of the G2-PAMAM-Ru catalyst for the reduction of **9**.

Recyclability of the catalyst has been successfully proven although decrease in catalytic activity has been observed in some cases. This proof-of-concept study has shown that judicious choice and optimization of solvents and reagents in terms of membrane<sup>19</sup> and dendrimer compatibility is important and is the key for the development of fully integrated continuous flow photochemical reactors with inline catalyst recovery.

## Notes and references

- (a) C. K. Prier, D. A. Rankic and D. W. C. MacMillan, *Chem. Rev.*, 2013, **113**, 5322; (b) R. A. Angnes, Z. Li, C. R. D. Correia and G. B. Hammond, *Org. Biomol. Chem.*, 2015, **13**, 9152; (c) J. M. R. Narayanam and C. R. J. Stephenson, *Chem. Soc. Rev.*, 2011, **40**, 102.
- S. Lin, M. A. Ischay, C. G. Fry and T. P. Yoon, *J. Am. Chem. Soc.*, 2011, **133**, 19350.



- 3 M. J. Schnermann and L. E. Overman, *Angew. Chem., Int. Ed.*, 2012, **51**, 9576.
- 4 (a) D. P. Hari and B. König, *Chem. Commun.*, 2014, **50**, 6688; (b) J. Zhao, W. Wu, J. Sun and S. Guo, *Chem. Soc. Rev.*, 2013, **42**, 5323.
- 5 (a) Y. Su, N. J. Straathof, V. Hessel and T. Noël, *Chem. – Eur. J.*, 2014, **20**, 10562; (b) Z. J. Garlets, J. D. Nguyen and C. R. J. Stephenson, *Isr. J. Chem.*, 2014, **54**, 351.
- 6 I. V. Gürsel, T. Noël, Q. Wang and V. Hessel, *Green Chem.*, 2015, **17**, 2012.
- 7 A. Kajetanowicz, J. Czaban, G. R. Krishnan, M. Malińska, K. Woźniak, H. Siddique, L. G. Peeva, A. G. Livingston and K. Grela, *ChemSusChem*, 2013, **6**, 182.
- 8 N. Priyadarshani, Y. Liang, J. Suriboot, H. S. Bazzi and D. E. Bergbreiter, *ACS Macro Lett.*, 2013, **2**, 571.
- 9 D. Rackl, P. Kreitmeier and O. Reiser, *Green Chem.*, 2016, **18**, 214.
- 10 J. F. B. Hall, X. Han, M. Poliakoff, R. A. Bourne and M. W. George, *Chem. Commun.*, 2012, **48**, 3073.
- 11 D. A. Tomalia, H. Baker, J. Dewald, M. Hall, G. Kallos, S. Martin, J. Roeck, J. Ryder and P. Smith, *Macromolecules*, 1986, **19**, 2466.
- 12 G. D. Storrer, K. Takada and H. C. D. Abruña, *Langmuir*, 1999, **15**, 872.
- 13 A. Ruggi, C. Beekman, D. Wasserberg, V. Subramaniam, D. N. Reinhoudt, F. W. B. van Leeuwen and A. H. Velders, *Chem. – Eur. J.*, 2011, **17**, 464.
- 14 (a) J. Guerra, A. C. Rodrigo, S. Merino, J. Tejeda, J. C. García-Martínez, P. Sánchez-Verdú, V. Ceña and J. Rodríguez-López, *Macromolecules*, 2013, **46**, 7316; (b) A. C. Rodrigo, I. Rivilla, F. C. Pérez-Martínez, S. Monteagudo, V. Ocaña, J. Guerra, J. C. García-Martínez, S. Merino, P. Sánchez-Verdú, V. Ceña and J. Rodríguez-López, *Biomacromolecules*, 2011, **12**, 1205.
- 15 F. R. Bou-Hamdan and P. H. Seeberger, *Chem. Sci.*, 2012, **3**, 1612.
- 16 R. Appel, *Angew. Chem., Int. Ed. Engl.*, 1975, **14**, 801.
- 17 C. Dai, J. M. R. Narayanam and C. R. J. Stephenson, *Nat. Chem.*, 2011, **3**, 140.
- 18 T. Hirao, J. Shiori and N. Okahata, *Bull. Chem. Soc. Jpn.*, 2004, **77**, 1763.
- 19 M. Janssen, C. Muller and D. Vogt, *Green Chem.*, 2011, **13**, 2247.

